Origin of Pressure-Induced Polyamorphism in $Ce_{75}Al_{25}$ Metallic Glass

Qiao-shi Zeng,[1,2] Yang Ding,[2] Wendy L. Mao,[1,3,4,5] Wenge Yang,[2,6] Stas. V. Sinogeikin,[6] Jinfu Shu,[7]
Ho-kwang Mao,[1,2,6,7] and J. Z. Jiang[1,*]

[1]*International Center for New-Structured Materials and Laboratory of New-Structured Materials,
Department of Materials Science and Engineering, Zhejiang University, Hangzhou 310027, China*
[2]*HPSynC, Carnegie Institution of Washington, Argonne, Illinois 60439, USA*
[3]*Geological & Environmental Sciences, Stanford University, Stanford, California 94305, USA*
[4]*Photon Science, SLAC National Accelerator Laboratory, Menlo Park, California 94025, USA*
[5]*Stanford Institute for Materials and Energy Science, SLAC National Accelerator Laboratory, Menlo Park, California 94025, USA*
[6]*HPCAT, Carnegie Institution of Washington, Argonne, Illinois 60439, USA*
[7]*Geophysical Laboratory, Carnegie Institution of Washington, Washington, D.C. 20015, USA*

Using high-pressure synchrotron x-ray absorption spectroscopy, we observed the Ce $4f$ electron in $Ce_{75}Al_{25}$ metallic glass transform from its ambient localized state to an itinerant state above 5 GPa. A parallel x-ray diffraction study revealed a volume collapse of about 8.6%, coinciding with $4f$ delocalization. The transition started from a low-density state below 1.5 GPa, went through continuous densification ending with a high-density state above 5 GPa. This new type of electronic polyamorphism in densely packed metallic glass is dictated by the Ce constituent, and is fundamentally distinct from the well-established structural polyamorphism in which densification is caused by coordination change and atomic rearrangement.

Metallic glasses have many unique properties which have put these materials at the cutting edge of materials research [1,2]. Their atomic packing, electronic behavior, and transition mechanism can be very different from other amorphous materials such as network-forming glasses. Pressure-induced polyamorphism [3] has been extensively reported in amorphous materials with directional and low coordination (<6) local environments, including amorphous ice [4,5], oxides [6–10], chalcogenides [11,12], silicon [13], and even single-component germanium metallic glass [14]. These structural polyamorphic transitions from a low-density amorphous (LDA) state to high-density amorphous (HDA) state often result from an increase in atomic coordination. Such coordination increase, and thus polyamorphism, was thought to be impossible in nondirectional, densely packed metallic glasses that already have the maximum coordination number (12–14) of random nearest neighbors [15]. Recently, surprising polyamorphic transitions were reported by Sheng *et al.* [16] and Yavari [17] in $Ce_{55}Al_{45}$ metallic glass and by Zeng *et al.* [18] in $La_{32}Ce_{32}Al_{16}Ni_5Cu_{15}$ bulk metallic glass based on the observation of kinks in the pressure shifts of the amorphous x-ray diffraction (XRD) peaks. The mechanism was suggested due to $4f$ electron delocalization in Ce under high pressure [16–18], which caused bond shortening and Kondo volume collapse [19,20]. This electronic polyamorphism is very different from the structural polyamorphism which involves coordination increase often coupled with bond lengthening (e.g., the Si-O and Ge-O bonds [7,8]). However, no direct experimental evidence on electronic changes has been reported, and the bond shortening was

modeled with the help of *ab initio* calculations [16]. It is also puzzling that the polyamorphic transition in $Ce_{55}Al_{45}$ metallic glass is smooth and continuous between 2 and 13.5 GPa, and has a large hysteresis loop upon the releasing pressure cycle below 2 GPa [16]. This behavior is different from the γ-α Ce $4f$ electronic delocalization transition which occurs sharply at 0.9 GPa without hysteresis [20], but is similar to the structural polyamorphism involving coordination rearrangement which characteristically occurs over a pressure range and shows considerable hysteresis [6,8]. The scatter in the data in Ref. [16] implies possible nonhydrostatic stresses in the sample, which may cause broadening of the observed transition region.

In the present Letter, we conducted diagnostic experiments to address these issues. To evaluate the connection between polyamorphism and Ce in the metallic glass, we used a metallic glass with the maximum possible Ce content and stayed with the Ce-Al binary to avoid possible complications that might arise from additional elements [18]. $Ce_{75}Al_{25}$ metallic glass ribbons with a thickness of about 15 μm and a width of about 1 mm were prepared using the single-roller melt spinning. Master ingots were prepared by arc melting a mixture of pure cerium (99.5 at. %) and aluminum (99.95 at. %) in a zirconium-gettered argon atmosphere. They were remelted 5 times to ensure homogeneity in composition. The samples were cut into about $50 \times 50 \times 12$ μm^3 chips, and then were loaded into a symmetrical diamond anvil cell (DAC) along with four tiny chips of ruby around the sample as a pressure calibrant [21]. The sample chamber was a 150 μm diameter hole drilled in a T301 stainless steel gasket (Fig. 1).

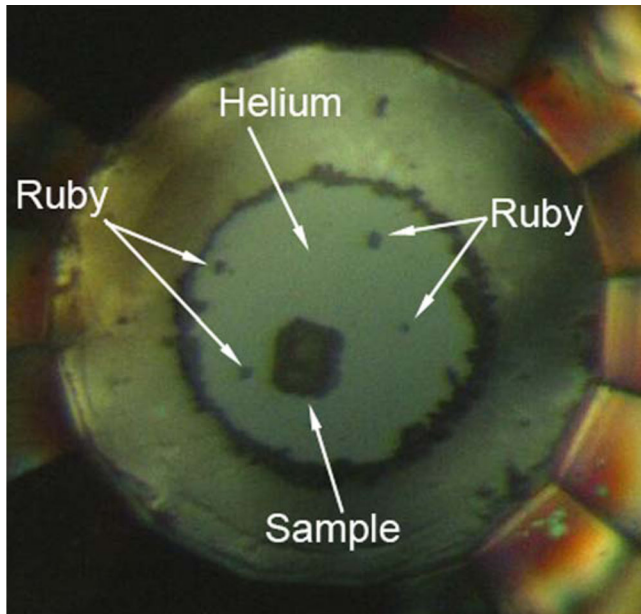FIG. 1 (color online).   Photomicrograph of sample loaded with helium in DAC at 0.8 GPa.

FIG. 2 (color online).   *In situ* high-pressure XRD patterns of $Ce_{75}Al_{25}$ metallic glass from 0.8 to 24.4 GPa. The position of FSDP shifts to the higher Q values with increasing pressure as a result of densification.

In situ high-pressure angle-dispersive XRD experiments with a focused x-ray beam of 15×15 μm^2 (FWHM) at a wavelength of 0.368 06 Å were performed at beam line 16ID-B and 16BM-D of the High Pressure Collaborative Access Team (HPCAT), Advanced Photon Source (APS), Argonne National Laboratory (ANL).

To evaluate the possible effect of nonhydrostatic stress on the observed broad transition region (2–13.5 GPa) and to improve the data quality, we loaded helium in the DAC as the pressure-transmitting medium, which provided the best hydrostatic condition to pressures above 100 GPa [22]. During the entire experiment, four chips of ruby showed well separated R_1-R_2 fluorescence peaks and identical pressure values, demonstrating excellent hydrostatic conditions. The pressure fluctuation during the XRD measurement, estimated from the pressures taken before and after exposure, was found to be less than 0.2 GPa. The XRD patterns were collected for 5 s at each pressure using a Mar345 image plate. Using the small 15×15 μm^2 focused x-ray beam to view the sample in the large 150 μm hole in the gasket, we completely avoided any XRD peak from the gasket. The single-crystal diamond anvils and helium pressure medium along the monochromatic x-ray beam path contributed very little background. Therefore, we were able to obtain the very clean XRD patterns required for characterization of the metallic glass which does not produce sharp peaks, but only broad features.

Figure 2 shows the series of XRD patterns at different hydrostatic pressures. Fifty XRD patterns were collected from ambient pressure to 24.4 GPa. The ambient pressure data was collected outside the DAC. The starting pressure in the DAC was 0.8 GPa in the fluid helium. With increasing pressure, the first sharp diffraction peak (FSDP) of the
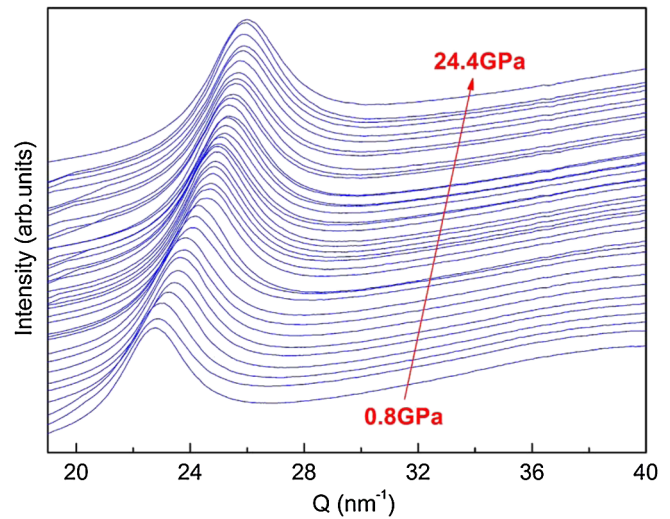
XRD pattern shifts towards high Q, as expected for the densification effect of pressure. The sample remained fully amorphous over the entire pressure range as indicated by the smooth patterns and absence of sharp Bragg peaks. The reverse FSDP position $2\pi/Q_1$ correlates with the volume of glass with a power law function [23,24], and can be conveniently used to estimate the relative volume (density) change under pressure using a Voigt line profile fitting after subtracting the baseline. We used the $1/3$ power law which is well established for volume estimation of amorphous materials under high temperatures [24] and pressures [7,8,25].

Figure 3 shows the inverse FSDP positions $2\pi/Q_1$ of $Ce_{75}Al_{25}$ metallic glass as a function of pressure. Two glassy states were distinctly separated by a transition region between 1.5 and 5 GPa with a large volume reduction of about 8.6% (2.9% in $2\pi/Q_1$) at ambient pressure, in which a power of $1/3$ was used to estimate the volume collapse, revealing a polyamorphic transition similar to the results reported by Sheng *et al.* [16]. The high quality data with small pressure uncertainty and small step size show very little scattering, and enable us to clearly distinguish three regions, i.e., the LDA below 1.5 GPa, the HDA above 5 GPa, and the intermediate-density amorphous (IDA) region between 1.5 and 5 GPa. We confirmed that the polyamorphic transition range is intrinsically broad even under hydrostatic conditions. The strong correlation between the transition pressures with the Ce contents, i.e., 2–13.5 GPa for the $Ce_{55}Al_{45}$ metallic glass, 1.5–5 GPa for the $Ce_{75}Al_{25}$ metallic glass, and 0.9 GPa for the pure crystalline Ce, clearly indicate that the polyamorphism is dictated by Ce. The large IDA region can be easily understood because unlike the crystalline solid α-γ Ce transition in which all Ce atoms have identical local environment and
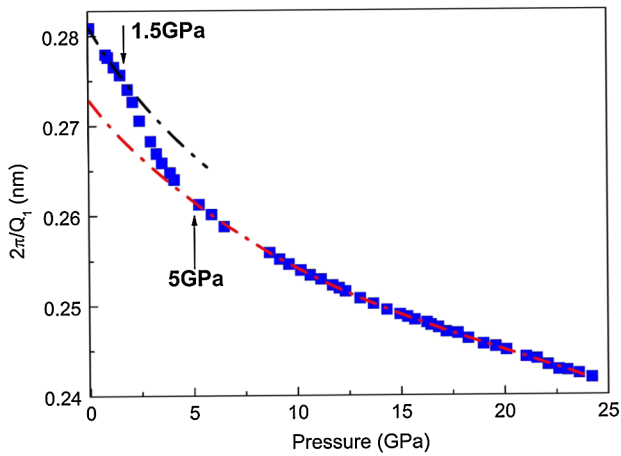
FIG. 3 (color online). Inverse FSDP positions $2\pi/Q_1$ of $Ce_{75}Al_{25}$ metallic glass as a function of pressure. Two distinct states, LDA (dashed black line) and HDA (dashed red line) along with a transition region from about 1.5 to 5 GPa can be identified. The data are smooth owing to the hydrostatic pressure conditions, and the pressure uncertainty is smaller than the symbol size.

FIG. 4 (color online). *In situ* high-pressure Ce L_3-edge XAS spectra of $Ce_{75}Al_{25}$ metallic glass. The arrows point to the $4f^0$ and $4f^1$ components. The appearance of the $4f^0$ feature indicates the delocalization of $4f$ electron, and coincides with the volume collapse in XRD results. The inset shows a schematic of the *in situ* high-pressure XAS experimental geometry.

transform in unison, each Ce atom in the binary glass encounters a random and different local environments and transforms differently over a pressure range.

The strongly correlated $4f$ electrons of Ce and their delocalization effects cause a lot of crystalline polymorphic transitions in pure elemental Ce and its alloys and compounds [19,20,26–28]. The same mechanism for pressure-induced polyamorphism transition was proposed in Ce-bearing metallic glasses by theoretical calculations [16,28], but direct experimental evidence was absent. X-ray spectroscopic methods have played a critical role in probing local structure and electronic changes in glasses at high pressure (e.g., [6,9]), but diamond absorption by the anvils rises steeply below 10 keV and effectively limits the range of elements and energies that can be studied. The Ce L_3 edge spectrum which provides the most definitive evidence for $4f$ delocalization requires energy down to 5.7 keV where the transmitted x ray is attenuated by 90% with every 500 μm thickness of diamond. A pair of conventional diamond anvils would be unusable allowing only 10^{-8} transmission at this energy. The problem was recently solved by using a pair of perforated diamonds capped by thin diamonds (2×500 μm total thickness), thus increasing the transmission to 10^{-2} allowing the $4f$ delocalization transition to be successfully studied in a DAC [29–31].

Here we used a different geometry in which the DAC was tilted by 18° to reduce the diamond in the optical path to 600 μm and maximize the transmission to 5% (Fig. 4, inset). We performed an *in situ* Ce L_3-edge x-ray absorption spectroscopy (XAS) experiment on $Ce_{75}Al_{25}$ metallic glass to monitor the $4f$ electronic structure change under high pressure. *In situ* high-pressure Ce L_3-edge XAS experiments were carried out at beam line 20BM-B, APS,
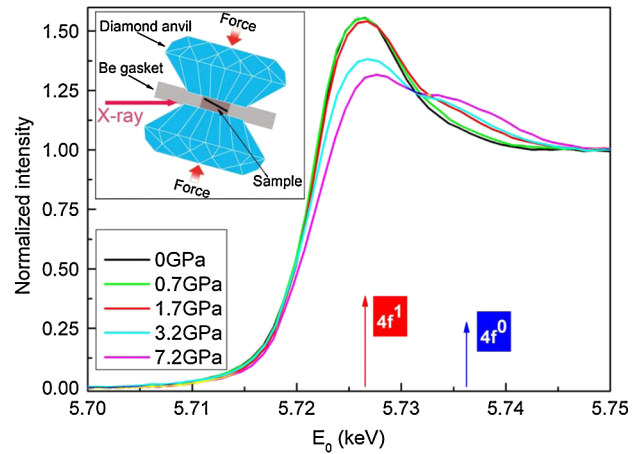
ANL. The transmission mode was employed with ion chambers filled with Ar-He gas mixture as the detectors. The beam size was about 12×6 μm^2. Samples were polished down to about 8 μm in thickness (the attenuation length is about 2.8 μm at the Ce L_3-edge, 5.724 keV) and were cut into $70 \times 70 \times 8$ μm^3 chips loaded in a panoramic DAC with an x-ray transparent Be gasket as the window material. The panoramic DAC had a 35° optical window in the axial direction through the diamond anvils, thus allowing the conventional pressure calibration with the ruby fluorescence method.

The Ce L_3-edge XAS spectra as a function of pressure are presented in Fig. 4. At ambient conditions, the spectrum exhibits only a $4f^1$ component, which basically shows a pure localized $4f$ configuration as expected. During compression, the postedge feature denoted itinerant $4f^0$ [29,30] appeared at about 10 eV higher energy than the $4f^1$ feature and grew with increasing pressure, while the intensity of $4f^1$ component decreased. The ratio of $4f^0$ to $4f^1$ components increased continuously over the intermediate region (1.7 and 3.2 GPa) and reached a plateau above 5 GPa, where the XAS spectra matched the fully itinerant state as documented in experiments and calculations of the crystalline γ-α Ce transition [30]. This clearly demonstrates the gradual and continuous delocalization of $4f$ electrons under high pressure, and coincides with the volume collapse in the pressure range of 1.5–5 GPa (Fig. 3). The result provides the direct experimental evidence of $4f$ electron delocalization for $Ce_{75}Al_{25}$ metallic glass, correlating with the pressure-induced LDA to HDA polyamorphism.

In conclusion, using *in situ* high-pressure XRD and XAS probes on a binary $Ce_{75}Al_{25}$ metallic glass under hydrostatic pressure conditions, we directly observed the onset

of a pressure-induced polyamorphic transition in LDA at 1.5 GPa, continuous transition in the intermediate pressure regime between 1.5 and 5 GPa, and complete transformation to HDA at 5 GPa. Densification in this novel type of polyamorphism is dictated by the Ce $4f$ electronic transition from localized to itinerant that causes volume collapse. This is fundamentally different from standard structural polyamorphism which is dictated by coordination changes and topological rearrangement of atoms. Understanding this new mechanism is valuable for searching for polyamorphism in other densely packed metallic glasses which contain Ce and other f metals with possible localized-itinerant electron transitions.

---

*jiangjz@zju.edu.cn

[1] A. L. Greer and E. Ma, MRS Bull. **32**, 611 (2007).
[2] D. B. Miracle, T. Egami, K. M. Flores, and K. F. Kelton, MRS Bull. **32**, 629 (2007).
[3] P. F. McMillan and M. C. Wilding, J. Non-Cryst. Solids **355**, 722 (2009).
[4] O. Mishima and Y. Suzuki, Nature (London) **419**, 599 (2002).
[5] C. A. Tulk, R. Hart, D. D. Klug, C. J. Benmore, and J. Neuefeind, Phys. Rev. Lett. **97**, 115503 (2006).
[6] J.-P. Itié *et al.*, Phys. Rev. Lett. **63**, 398 (1989).
[7] C. Meade, R. J. Hemley, and H. K. Mao, Phys. Rev. Lett. **69**, 1387 (1992).
[8] M. Guthrie *et al.*, Phys. Rev. Lett. **93**, 115502 (2004).
[9] S. K. Lee, P. J. Eng, H. K. Mao, Y. Meng, and J. Shu, Phys. Rev. Lett. **98**, 105502 (2007).
[10] E. Soignard, S. A. Amin, Q. Mei, C. J. Benmore, and J. L. Yarger, Phys. Rev. B **77**, 144113 (2008).
[11] W. A. Crichton, M. Mezouar, T. Grande, S. Stolen, and A. Grzechnik, Nature (London) **414**, 622 (2001).
[12] Q. Mei *et al.*, Phys. Rev. B **74**, 014203 (2006).
[13] P. F. McMillan, M. Wilson, D. Daisenberger, and D. Machon, Nature Mater. **4**, 680 (2005).
[14] M. H. Bhat *et al.*, Nature (London) **448**, 787 (2007).
[15] H. W. Sheng, W. K. Luo, F. M. Alamgir, J. M. Bai, and E. Ma, Nature (London) **439**, 419 (2006).
[16] H. W. Sheng *et al.*, Nature Mater. **6**, 192 (2007).
[17] A. R. Yavari, Nature Mater. **6**, 181 (2007).
[18] Q. S. Zeng *et al.*, Proc. Natl. Acad. Sci. U.S.A. **104**, 13 565 (2007).
[19] J. W. Allen and R. M. Martin, Phys. Rev. Lett. **49**, 1106 (1982).
[20] M. J. Lipp *et al.*, Phys. Rev. Lett. **101**, 165703 (2008).
[21] H. K. Mao, J. Xu, and P. M. Bell, J. Geophys. Res. **91**, 4673 (1986).
[22] P. Loubeyre *et al.*, Nature (London) **383**, 702 (1996).
[23] D. Ma, A. D. Stoica, and X. L. Wang, Nature Mater. **8**, 30 (2009).
[24] A. R. Yavari *et al.*, Acta Mater. **53**, 1611 (2005).
[25] J. Z. Jiang *et al.*, Appl. Phys. Lett. **84**, 1871 (2004).
[26] Y. Y. Chen *et al.*, Phys. Rev. Lett. **84**, 4990 (2000).
[27] B. Johansson, I. A. Abrikosov, M. Aldén, A. V. Ruban, and H. L. Skriver, Phys. Rev. Lett. **74**, 2335 (1995).
[28] Q. S. Zeng *et al.*, Proc. Natl. Acad. Sci. U.S.A. **106**, 2515 (2009).
[29] J.-P. Rueff *et al.*, Phys. Rev. Lett. **93**, 067402 (2004).
[30] J. P. Rueff *et al.*, Phys. Rev. Lett. **96**, 237403 (2006).
[31] J. P. Itié *et al.*, J. Phys. Condens. Matter **17**, S883 (2005).